한국소음진동공학회 2003년도 춘계학술대회논문집, pp.368~373.

균일힘 액추에이터와 가속도계 배열을 이용한 지능구조물의 능동구조 음향제어

Active Structural Acoustical Control of a Smart Structure using Uniform Force Actuator and Array of Accelerometers

이영섭*·Stephen J Elliott**·Paolo Gardonio**

Young-Sup Lee, Stephen J Elliott and Paolo Gargonio

Key Words : Active Structural Acoustical Control (능동구조음향제어), Piezoelectric Transducers (압전트랜스듀서), Matched Sensor and Actuator (매치된 센서 및 액추에이터), Direct Velocity Feedback (직접속도피드백), Smart Panel (스마트판넬).

ABSTRACT

This paper presents a study of low frequencies volume velocity vibration control of a smart panel in order to reduce sound transmission. A distributed piezoelectric quadratically shaped polyvinylidene fluoride (PVDF) polymer film is used as a uniform force actuator and an array of 4×4 accelerometer is used as a volume velocity sensor for the implementation of a single-input single-output control system. The theoretical and experimental study of sensor-actuator frequency response function shows that this sensor-actuator arrangement provides a required strictly positive real frequency response function below about 900 Hz. Direct velocity feedback could therefore be implemented with a limited gain which gives reductions of about 15 dB in vibration level and about 8 dB in acoustic power level at the (1,1) mode of the smart panel. It has been also shown that the shaping error of PVDF actuator could limit the stability and performance of the control system.

1. Introduction

Active control methods have been applied effectively for low frequency noise control.[1,2] This method can be used for the sound radiation/transmission control of a panel. This paper presents a theoretical and experimental study of low frequency feedback control of sound transmission through a panel based on active structural acoustical control (ASAC).[2]

ASAC systems [2] utilize structural actuators that are driven to minimize the overall sound radiation/transmission of the panel that could be either estimated with a set of acoustic sensors placed in the radiating area or indirectly with structural sensors.

Johnson and Elliott [3] have shown that the net volume velocity of a panel is a good estimator of the low frequency sound radiation.

Volume velocity has been measured in practice using structural sensors, as for example arrays of quadratically shaped polyvinylidene fluoride (PVDF) polymer strips [3,4], variable width PVDF strips[5] and arrays of piezoelectric patches[6]. These structural sensors provide a single output proportional to the volume velocity vibration of a panel that could be used to implement single channel direct velocity feedback control (DVFB) using a matched and collocated uniform force piezoelectric actuator.[7]

A feedback control system with a collocated actuator-sensor could give considerable advantages for DVFB, such as robust stability and high performance.[8] However a *matched* piezoelectric sensor/actuator pair has been found that the transfer function of a matched piezoelectric actuator/sensor pair does not provide strictly positive real (SPR) property due to *in-plane motion coupling* with the transverse motion.[7,9] Although several solutions to this problem have been suggested, they have not been successful.

Maillard and Fuller[10] have suggested to measure volume velocity vibration with an array of accelerometers so that the in-plane coupling phenomenon for the detection of volume velocity is avoided. For this study, a

* 한국표준과학연구원
E-mail : yslee@kriss.re.kr
Tel : (042) 868-5705, Fax : (042) 868-5639

** ISVR, University of Southampton, UK

smart panel with a uniform force strain actuator made with a quadratically shaped PVDF film on one side and an array of accelerometers-sensors on the other side has been constructed.

Because this paper targets to study a single-input single-output (SISO) control system, which is simple and easily implementable in real applications required by industries, the control system adopts a simple DVFB strategy.

The theoretical description on the quadratically shaped PVDF actuator and the volume velocity sensor used in this study is given in section 2. Section 3 describes the modelling of a SISO feedback controller and the plant. Section 4 discusses the experimental results on the vibration and acoustic feedback control of the smart panel.

2. Design of Actuator and Sensor

2.1 Uniform Force Actuator

The *out-of-plane uniform force actuator* can be regarded as a composite structure consisting of piezoelectric film with very thin electrodes on both sides. When the piezoelectric actuator is excited by an input voltage $V_3(t)$, after some manipulation, the forced equation for the out-of-plane motion of the panel can be derived as[9]

$$(D_s + D_{pe})\left(\frac{\partial^4 w}{\partial x^4} + 2\frac{\partial^4 w}{\partial x^2 \partial y^2} + \frac{\partial^4 w}{\partial y^4}\right) + m\frac{\partial^2 w(t)}{\partial t^2} = -h_{act} V_3(t) L_{pe}[S(x,y)] + p(x,y,t) \quad (1)$$

where D_s and D_{pe} are the flexural rigidity, $h_{act} = h_s + h_{pe}/2$ and and $p(x,y,t)$ is the distributed out-of-plane loading. The space differential operator describing the transverse excitation on the panel is given by

$$L_{pe}[S(x,y)] = e_{31}\frac{\partial^2 S(x,y)}{\partial x^2} + 2e_{36}\frac{\partial^2 S(x,y)}{\partial x \partial y} + e_{32}\frac{\partial^2 S(x,y)}{\partial y^2} \quad (2)$$

The condition necessary to generate an out-of-plane uniform force is to have a constant sensitivity function along the y-direction and quadratic sensitivity along the x-direction[9]:

$$S(x,y) = -k(x^2 - L_x x) \quad (3)$$

where k is a constant so that the boundary conditions $S(0,y) = 0$ and $S(L_x,y) = 0$. It can be found that $\partial^2 S(x,y)/\partial x^2 = \text{constant} = -2k$ and $k = 4L_y/L_x^2$. The resulting distributed out-of-plane uniform force $f_u(t)$, per unit surface area is expressed as[9]

$$f_u(t) = -h_{act} V_3(t) L_{pe}[S(x,y)] = 2h_{act} e_{31} k V_3(t) \quad (4)$$

When $e_{31} = 0.052$ [$NV^{-1}m^{-1}$], k=16.903 (when $L_x = 0.313$ m and $L_y = 0.414$ m. Refer the properties of the panel and PVDF film.) and h_{act}=0.00075 [m].

Table 1 Physical properties of the panel and film.

	panel	PVDF film
Dimension (length× width)	$L_x \times L_y$ = 313×414 mm (aluminum)	$L_x \times \Delta L_y$ = 313×10 mm (Forty quadratically shaped strips)
Thickness	$2h_s$ = 1 mm	h_{pe} = 0.5 mm
Mass density	ρ_s = 2700 kgm^{-3}	ρ_{pe} = 1780 kgm^{-3}
Young's modulus	$Y_s = 7.1\times10^{10}$ Nm^{-2}	$Y_{pe} = 2.0\times10^{9}$ Nm^{-2}
Poisson ratio	ν_s = 0.33	ν_{pe} = 0.31
Histeresis loss factor	η_s = 0.05	η_{pe} = 0.05

In implementation, as Rex and Elliott[4] suggested, a number of PVDF strips are bonded on the plate in order to approximate a quadratic sensitivity in the x direction as shown in Fig. 1.

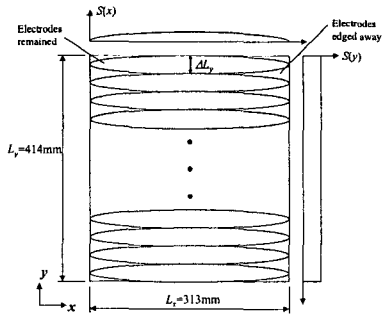

Fig. 1 Arrangement of a matched quadratic piezoelectric PVDF actuator and sensor pair.

This type of actuator can approximate a uniform force if the width ΔL_y of each strip is sufficiently small compared with the structural wavelength of the panel. In this panel, 40 PVDF strips are implemented and each strip is 10 mm wide. The shape constant of each strip

is $k_\Delta = 4\Delta L_y / L_x^2$, which satisfies $k = 40k_\Delta$. The pressure amplitude 0.13 Pa of the uniform force actuator at 100V is equivalent to about 76 dB in terms of sound pressure level.

2.2 Accelerometers Array

The volume velocity of a harmonically vibrating plate ($L_x \times L_y \times 2h_s$) is expressed analytically as

$$Q(\omega) = j\omega\left[\int_0^{L_x}\int_0^{L_y} w(x,y,\omega)dxdy\right], \quad (5)$$

where $w(x,y,\omega)$ is the flexural displacement of the plate. As suggested by Maillard and Fuller[10], an array of 16 accelerometers evenly distributed over the panel surface has been used to reconstruct the volume velocity of the panel as

$$\tilde{Q}(\omega) = \sum_{k=1}^{16} v_k(x_k, y_k, \omega), \quad (6)$$

The 16 accelerometers are arranged to make a 4×4 array every 1/8, 3/8, 5/8, 7/8 of L_x and L_y of the smart panel. This arrangement is adapted in order to avoid the in-plane coupling problem between the sensor and the actuator. As described in references[7,9], the measured FRF with the matched PVDF sensor/actuator pair as shown in Fig. 2, suffers from the coupling due to in-plane vibration.

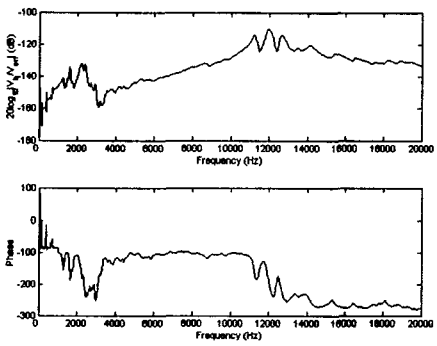

Fig. 2 Measured FRF of the matched PVDF sensor/actuator pair with the coupling problem.

The in-plane coupling can be characterized as an increasing trend of magnitude with the increase of frequency, and a phase lag at about 12000 Hz that exceeds −90° so that the sensor-actuator FRF is not SPR[9], which cannot provide unconditional stability of the DVFB control scheme.

3. Modelling of Controller and Plant

3.1 SISO Feedback Controller

The panel with the 4×4 array of accelerometers and the piezoelectric actuator is clamped on a wooden box as can be seen from Fig. 3. A loudspeaker is installed inside the box to generate primary disturbance noise on the panel. The 16 accelerometers (PCB A352C67) are connected to a PCB 481A signal conditioner that sums all the 16 signals together. This signal is then integrated through a PCB 480B10 integrator to generate a velocity signal. The resulting SISO sensor/actuator system has been connected to a SISO feedback controller.

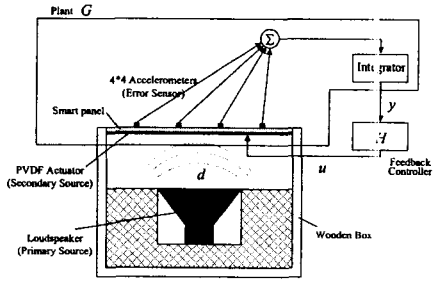

Fig. 3 Experimental set-up of a smart panel with the PVDF actuator and accelerometer array.

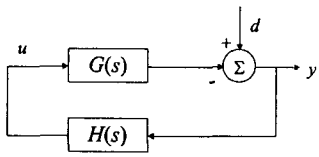

Fig. 4 Velocity feedback control scheme.

As shown in Fig. 4, the system is composed of a smart panel characterized by its plant response $G(s)$, a controller $H(s)$ and a primary source (loudspeaker). The plant $G(s)$ includes the panel, a secondary source (PVDF actuator) and an error sensor (accelerometer array). If the feedback control system is stable, the spectrum of the error sensor output $y(j\omega)$ is related to that of the sensor output before control, $d(j\omega)$, by the expression[8]

$$y(j\omega)=[1+G(j\omega)H(j\omega)]^{-1}d(j\omega), \quad (7)$$

For this control scheme, the control input to the secondary source (actuator) is given by $u(j\omega)=H(j\omega)[1+G(j\omega)H(j\omega)]^{-1}d(j\omega)$.[8] For the DVFB control strategy, the controller is assumed to be a constant gain, so that $H(j\omega)=h$, where h is the feedback gain. Thus if FRFs of the plant of the sensor-actuator and the controller are both SPR so that the velocity feedback control system in Fig. 4 is *unconditionally stable*. Therefore the feedback gain can be increased, in principle, to infinity in order to drive to zero the signal from the control sensor.

In practice, the system under study only approximates a volume velocity sensor and uniform force actuator so that its open-loop FRF $G(j\omega)H(j\omega)$ has to be analyzed with reference to the Nyquist stability condition.

3.2 Analytical Modelling of the Plant

When the panel is clamped (C-C-C-C) and subject to transverse vibration, the harmonic out-of-plane velocity at the $k-th$ accelerometer point of K points on the panel [See Table 1.] can be given as

$$v_k(x_k,y_k,\omega)=j\omega\sum_{m,n}B_{mn}(\omega)\phi_{mn}(x_k,y_k), \quad (8)$$

where for a uniform out-of-plane force excitation $f_u(\omega)$, the modal amplitude $B_{mn}(\omega)$ is given by

$$B_{mn}(\omega)=\frac{\int_0^{L_y}\int_0^{L_x}f_u(\omega)\phi_{mn}(x,y)dxdy}{\Lambda_{mn}[\omega_{mn}^2(1+j\eta_s)-\omega^2]}, \quad (9)$$

where η_s is the hysteresis loss factor of the panel and the normalization factor Λ_{mn} can be written as[9]

$$\Lambda_{mn}=\rho_s(2h_s)^2\int_0^{L_y}\int_0^{L_x}\phi_{mn}^2(x,y)dxdy=\rho_s h_s^2 L_x L_y, \quad (10)$$

The $m,n-th$ out-of-plane natural frequency ω_{mn} of the panel is expressed as[9]

$$\omega_{mn}=\frac{\pi^2 h_s}{L_y^2}\left\{\frac{Y_s\alpha}{3\rho_s(1-\nu_s^2)}\right\}^{1/2}, \quad (11)$$

where α is given by ref.(9).

The harmonic out-of-plane velocity can be rewritten as

$$v_k(x_k,y_k,\omega)=j\omega\sum_{m,n}f_u(\omega)C_{mn}D_{mn}\phi_{mn}(x_k,y_k), \quad (12)$$

where $C_{mn}=\int_0^{L_y}\int_0^{L_x}\phi_{mn}(x,y)dxdy$ and $D_{mn}=\frac{1}{\Lambda_{mn}[\omega_{mn}^2(1+j\eta_s)-\omega^2]}$. The out-of-plane mode of the panel can be calculated by the product of the two beam functions, $\phi_{mn}(x_k,y_k)=\phi_m(x_k)\phi_n(y_k)$, as described in the ref. (9). After some manipulation, the coefficient C_{mn} has been found to be[9] :

$$C_{mn}=\frac{16L_xL_y}{\gamma_m\gamma_n}\sin\left(\frac{\gamma_m}{2}\right)\sin\left(\frac{\gamma_n}{2}\right), \quad (13)$$

where $m,n=1,3,5,...$ and the constant γ_i can be calculated with ref.(9). Thus the plant of the system can be analytically expressed with

$$G(\omega)=\tilde{Q}(\omega)/V_3(\omega) \quad (14)$$
$$=-h_{act}L_{pe}[S(x,y)]\sum_{k=1}^{K}\left[j\omega\sum_{m,n}C_{mn}D_{mn}\phi_{mn}(x_k,y_k)\right]$$

4. Experiment and Result

4.1 FRF of the Plant

As plotted in Fig. 5, the measured plant FRF, i.e. output sum of velocities per unit input voltage to the uniform force actuator, shows rhe accelerometers array sensor does not suffer from in-plane coupling. Thus Fig. 5 measured with accelerometer array sensor can measure a much larger number of out-of-plane resonances compared to that of the matched piezosensor shown in Fig. 2.

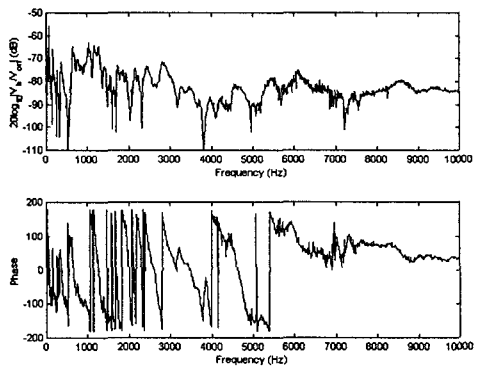

Fig. 5 Measured FRF of the PVDF actuator and accelerometers array at 0 ~10000Hz.

A gradual decreasing magnitude trend with the increase of frequency up to 10000 Hz can be found. It is also found that the plant FRF with the configuration of the PVDF actuator and the 4×4 accelerometer array is not coupled via in-plane vibration of the panel. The sensor-actuator FRF at a lower frequency range is plotted in Fig. 6. Since some shaping errors have been highlighted for the quadratic electrodes of the PVDF actuator, the measured (*thick line*) and calculated (designed actuator shape: *dashed line*, erroneous actuator shape: *thin line*) plant FRFs between 0 and 2000 Hz are compared as shown in Fig. 6.

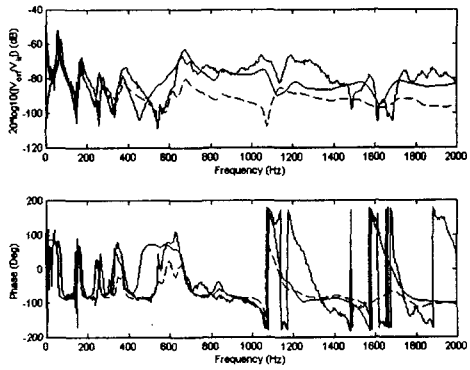

Fig. 6 Measured FRF of the PVDF actuator and accelerometers array at 0 ~2000Hz.

The calculated plant FRF with the designed PVDF actuator shape shows a continuous reduction of the magnitude with frequency. The phase response lies between ±90° up to about 900 Hz. Above 900 Hz the phase response is characterized by a phase lag with an anti-resonance at the frequency of about 1100 Hz. This is caused by aliasing problems due to the limited number of accelerometers used to reconstruct the volume velocity. The measured FRF shows the typical feature of driving point mobility below about 350 Hz, which includes the first three odd bending modes of the panel that largely contribute to the low frequency sound radiation. The resonances are alternated by anti-resonances that occur at frequencies quite close to the following resonance. Also the phase response lies between ±90° and the magnitude tends to decrease with frequency. However, the measured FRF between about 350 Hz and 900 Hz shows two unexpected higher peaks in correspondence to the resonance frequencies of the fourth and fifth modes. Beyond about 900 Hz, the measured sensor-actuator FRF is characterized by sharp resonances with phase lags. The two sharp resonances located at about 1000 Hz - 1200 Hz are high enough to cause instability of the feedback control system when a high feedback gain is used. The calculated FRF with the erroneous shaped actuator shows a similar trend to the measured one.

Thus the configuration of the smart panel with the PVDF actuator having shaping errors, and an array of 4×4 accelerometers gives SPR property below about 900 Hz so that a *conditionally stable* SISO controller only can be implemented. The feedback gain in the control system must be limited because of the two sharp peaks at about 1000 - 1200 Hz.

4.2 Acoustical Control using Velocity Feedback

Since the smart panel can not provide SPR property at all frequencies, a limited positive feedback gain is chosen to implement a conditionally stable feedback controller. Figure 8 shows the measured volume velocity with (*dashed line*) and without (*solid line*) control when the panel is excited with the acoustic field (white noise) generated by the loudspeaker in the wooden box.

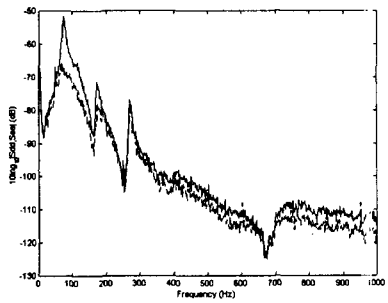

Fig. 7 Measured vibration control result. Before control: *dashed line* and after control: *solid line*.

The volume velocity attenuation of about 15 dB at the resonance frequency of the first mode has been achieved when the gain margin is 6dB. The volume velocity attenuation for resonance of the second mode is about 6 dB and that of the third mode is about 5 dB. The attenuation between the resonance of the third mode and 1000 Hz is of the order of about 5

dB as well.

The sound transmission control experiment has been carried out with the same feedback gain. In this experiment, a B&K Type 4165 1/2" microphone, which microphone has been installed about 10cm above the panel in correspondence to its center, has been used to measure the radiated sound pressure from the panel. Figure 10 shows the measured sound pressure with (*dashed line*) and without (*solid line*) control. The attenuation of the sound transmission for the resonance frequency of the first mode is about 8 dB and about 5 dB for both the second and third modes. The controlled FRF between the third mode and about 800 Hz maintains small attenuation as well, however the enhancement has been found at higher frequencies, especially at the resonances in about 800 – 900 Hz.

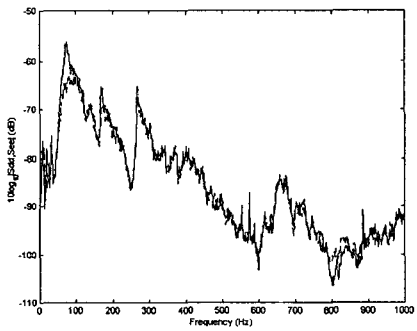

Fig. 8 Measured acoustic control result. Before control: *dashed line* and after control: *solid line*.

Since the sound transmission control has been carried out with the smart panel clamped on a wooden box in a general experimental lab, more exact measurement could be achieved when the testing rig is used in an anechoic chamber. In this acoustic transmission test, as shown in Figure 3, the cavity below the panel in the box is about 420mm(L) × 320mm(B) × 120mm(D). The first cross resonance of the cavity occurs at about 290 Hz, and so the pressure distribution in the cavity below the plate will be strongly non-uniform above this frequency.

The acoustic transmission control results are rather modest compared with those in terms of volume velocity. This is probably due to the test being conducted in a reverberant laboratory despite since in theory volume velocity is directly proportional to far-field sound pressure on the z axis.The attenuation measured with this experiment could be improved by the use of a phase lag compensator, which could modify the open-loop FRF of the plant at the frequency range about 1000 – 1200 Hz. For reference, the overall reduction in vibration level of about 3.4 dB and pressure level of about 0.2 dB up to 1000 Hz has been achieved.

5. Conclusions

This paper reports a study of low frequencies volume velocity control of a smart panel for the reduction of sound transmission through a smart panel. The smart panel is a clamped aluminum rectangular plate with the dimension of 414×313×1 mm. The panel has an array of quadratically shaped PVDF actuators and an array of 4×4 accelerometers with a SISO DVFB control system. With a direct velocity feedback control, the attenuations of about 15 dB in vibration level and about 8 dB in acoustic power level at the resonance frequency of the first mode of the smart panel have been achieved.

References

(1) P. A. Nelson and S. J. Elliott, 1992, *Active Control of Sound*, Academic Press.

(2) C. R. Fuller, S. J. Elliott, and P. A. Nelson, 1996, *Active Control of Vibration*, Academic Press.

(3) M. E. Johnson and S. J. Elliott, 1995, *Journal of Acoustical Society of America*, 98(4), 2174-2186, Active control of sound radiation using volume velocity cancellation.

(4) J. Rex and S. J. Elliott, 1992, *Proceedings of MOVIC*, 339-343, The QWSIS-A new sensor for structural radiation control.

(5) F. Charette, A. Berry, and C. Guigou, 1998, *Journal of the Acoustical Society of America*, 103(3), 1493-1503, Active control of sound radiation from a plate using a polyvinylidene fluoride volume displacement sensor.

(6) A. Preumont, A. Francois, and S. Debru, 1999, *ASME Journal of Vibration and Acoustics*, 121, 446-452, Piezoelectric array sensing for real-time, broad-band sound radiation measurement.

(7) P. Gardonio, Y.-S. Lee, S. J. Elliott, and S. Debost, 2001, *Journal of the Acoustical Society of America*, 110, 6, 3025-3031, Analysis and measurement of a matched volume velocity sensor and uniform force actuator for active structural acoustic control.

(8) S. J. Elliott, 2001, *Signal Processing for Active Control*, Academic Press.

(9) Y.-S. Lee, 2000, *Active control of smart structures using distributed piezoelectric transducers*, PhD thesis, University of Southampton.

(10) J. P. Maillard and C. R. Fuller, 1998, *Journal of Acoustical Society of America*, 103(1), 396 – 400, Comparison of two structural sensing approaches for active structural acoustic control.